

## Research Article

Theme: Translational Application of Nano Delivery Systems: Emerging Cancer Therapy  
Guest Editors: Mahavir B. Chougule and Chalet Tan

# Characterization and Evaluation of 5-Fluorouracil-Loaded Solid Lipid Nanoparticles Prepared *via* a Temperature-Modulated Solidification Technique

Meghavi N. Patel,<sup>1</sup> Sushant Lakkadwala,<sup>1</sup> Mohamed S. Majrad,<sup>1</sup> Elisha R. Injeti,<sup>2</sup> Steven M. Gollmer,<sup>3</sup> Zahoor A. Shah,<sup>4</sup> Sai Hanuman Sagar Boddu,<sup>1</sup> and Jerry Nesamony<sup>1,5</sup>

Received 28 October 2013; accepted 14 May 2014; published online 18 July 2014

**Abstract.** The aim of this research was to advance solid lipid nanoparticle (SLN) preparation methodology by preparing glyceryl monostearate (GMS) nanoparticles using a temperature-modulated solidification process. The technique was reproducible and prepared nanoparticles without the need of organic solvents. An anticancer agent, 5-fluorouracil (5-FU), was incorporated in the SLNs. The SLNs were characterized by particle size analysis, zeta potential analysis, differential scanning calorimetry (DSC), infrared spectroscopy, atomic force microscopy (AFM), transmission electron microscopy (TEM), drug encapsulation efficiency, *in vitro* drug release, and *in vitro* cell viability studies. Particle size of the SLN dispersion was below 100 nm, and that of redispersed lyophilizates was ~500 nm. DSC and infrared spectroscopy suggested that the degree of crystallinity did not decrease appreciably when compared to GMS. TEM and AFM images showed well-defined spherical to oval particles. The drug encapsulation efficiency was found to be approximately 46%. *In vitro* drug release studies showed that 80% of the encapsulated drug was released within 1 h. *In vitro* cell cultures were biocompatible with blank SLNs but demonstrated concentration-dependent changes in cell viability to 5-FU-loaded SLNs. The 5-FU-loaded SLNs can potentially be utilized in an anticancer drug delivery system.

**KEY WORDS:** atomic force microscopy; calorimetry (DSC); FTIR; particle size; solid lipid nanoparticles.

## INTRODUCTION

Colloidal drug delivery systems, namely, oil-in-water emulsions, liposomes, micelles, microparticles, and nanoparticles, offer new opportunities for targeting drugs and pharmaceuticals (1–3). Solid lipid nanoparticles (SLNs) have demonstrated superiority in certain aspects over other types of colloidal carriers (4). SLNs consist of spherical lipid particles in the nanometer size range. They offer several advantages in drug delivery due to their small particle size, large surface area, and ability to modify their surface properties easily. SLNs are used for controlled and targeted delivery, to

improve bioavailability, to improve drug stability against enzymatic degradation, and for the incorporation of hydrophilic and lipophilic drugs (5).

Recently, several research groups have developed SLN technology as an alternative to other colloidal carriers, and their studies improved methods for preparing SLNs (1,6,7). The most prevalent production technique used to prepare SLNs is *via* high-pressure homogenization. However, some potential disadvantages of this process are chances of metal contamination, high polydispersity, thermal degradation of sensitive drugs, and the presence of supercooled melts (4). Two other widely used production techniques are the microemulsion method (8) and the solvent evaporation by precipitation in o/w emulsions (9). The microemulsion method is highly sensitive to minor changes in composition and thermodynamic variables. The solvent evaporation method utilizes organic solvents that are toxic and harmful to the environment. Therefore, there is a need for a simple, robust, less energy-consuming, and organic solvent-free method that is easy to scale up for large-scale SLN production. This was the rationale to develop the temperature-modulated solidification method for preparing SLNs reported in this research work.

An area of application that is being researched extensively using SLN-based formulations is anticancer drug delivery. Hydrophilic and lipophilic anticancer agents have been incorporated in SLNs (10,11). SLNs facilitate formulation of lipophilic and poorly water-soluble drugs and hence will enable

<sup>1</sup> Department of Pharmacy Practice, College of Pharmacy and Pharmaceutical Sciences, University of Toledo, 3000 Arlington Avenue, MS1013, Toledo, Ohio 43614, USA.

<sup>2</sup> Department of Pharmaceutical Sciences, School of Pharmacy, Cedarville University, 251N. Main St., Cedarville, Ohio 45314, USA.

<sup>3</sup> Department of Science and Mathematics, College of Arts and Sciences, Cedarville University, 251 N. Main St., Cedarville, Ohio 45314, USA.

<sup>4</sup> Department of Medicinal and Biological Chemistry, College of Pharmacy and Pharmaceutical Sciences, University of Toledo, 3000 Arlington Avenue, MS1013, Toledo, Ohio 43614, USA.

<sup>5</sup> To whom correspondence should be addressed. (e-mail: jerry.nesamony@utoledo.edu)

delivering such drugs through otherwise unfeasible routes of administration. Chemotherapeutic agents used in primary and palliative care of various cancers are normally administered intravenously. The chemotherapeutic regimen is intensive and involves multiple agents. As soon as chemotherapy is initiated, severe side effects such as nausea and vomiting, alopecia, *etc.* occur in patients. Thus, additional pharmacologic agents have to be administered to minimize patient discomfort and promote adherence. High doses of anticancer agents are given intravenously to maintain a therapeutic concentration of the drug at the cancerous lesion. However, blood carries these agents to healthy tissues and organs, producing undesirable side effects. In addition to these challenges, cancer cells tend to develop resistance to cancer drugs, leading to decreased therapeutic efficacy. SLN-based anticancer drug delivery has demonstrated the ability to address many of these challenges in *in vitro* experiments, cell and tissue culture studies, and animal testing (10–12). This is the rationale to incorporate an anticancer agent in the developed SLNs for future potential application in colorectal cancer therapy. Although colorectal cancer is treatable surgically, recurrence following surgery is a major problem and in general leads to poor prognosis and high mortality (13,14). There is currently a need to advance the therapeutic options and formulations available to treat colorectal cancer.

The aim of the present study was to investigate the feasibility of preparing glyceryl monostearate (GMS) nanoparticles by using a novel temperature-modulated solidification process and to evaluate its potential as an anticancer drug delivery system. 5-Fluorouracil (5-FU), an anticancer drug, was incorporated as a model drug in the SLNs. 5-FU is an antimetabolite chemotherapeutic agent used in chemotherapy of colorectal, stomach, breast, and pancreatic cancer (15). It is used topically in the form of a cream for the treatment of actinic (solar) keratoses and some basal cell carcinomas of the skin (16). 5-FU is an analog of naturally occurring pyrimidine uracil, and it is metabolized *via* the same metabolic pathways as uracil (17). As a pyrimidine analog, it is transformed inside the cell into various cytotoxic metabolites. The latter are then incorporated into DNA and RNA, finally inducing cell cycle arrest and apoptosis by inhibiting the cell's ability to synthesize DNA (16,18).

## MATERIALS

GMS and D-trehalose, anhydrous, acetonitrile (HPLC grade) and ethanol (HPLC grade) were purchased from Fisher Scientific (Pittsburg, PA); Tween 80 (polyoxyethylene (19) sorbitan monooleate) and 5-FU were purchased from Spectrum Chemical Manufacturing Corporation (New Brunswick, NJ), and Amicon Ultra-15 centrifugal filter units were purchased from EMD Millipore (Billerica, MA). Deionized water was obtained from the central deionized water line in our laboratory.

## METHODS

### Preparation of 5-FU-Loaded SLNs

An accurately weighed quantity of 5-FU was added to 1 g of GMS and equilibrated at 75°C for 48 h at 1,500 rpm after

placing in a thermostated shaker. Tween 80 was added to the drug-GMS mixture and vortexed to obtain a homogenous dispersion. Deionized water was heated to the same temperature as the molten lipid phase. The molten lipid phase was then dispersed into the heated deionized water, placed in an ice bath, and stirred at 4,000 rpm for 45 min by a high-shear mixer (model L5M-A, Silverson, USA). The resulting SLN dispersion was used for further characterization. To isolate the SLNs, an aliquot of the aqueous SLN dispersion was placed in a 100-kDa Amicon Ultra-15 centrifugal filter unit and centrifuged at 7,830 rpm for 30 min and temperature-maintained at 15°C in a centrifuge 5430R (Eppendorf AG, Hamburg, Germany). The SLNs retained by the filter were collected and redispersed in deionized water before lyophilization. Anhydrous trehalose, equivalent to the amount of GMS, was used as cryoprotectant. The mixture was frozen quickly at –75°C in a freezer and lyophilized for 72 h in the lyophilizer (FreeZone 2.5-1 benchtop freeze dry system, Labconco, MO, USA) at –49°C and vacuum-maintained at 0.120 mBar. SLNs with no added drug were prepared by an identical procedure after excluding the drug addition step. The lyophilized samples were collected and stored in a desiccator for further characterization.

### Drug Encapsulation Efficiency

An aliquot of lyophilized 5-FU-loaded SLNs was dissolved in 5 ml 50/50 HPLC-grade ethanol/HPLC-grade water and vortexed at 3,000 rpm. The solution was then filtered through a 0.45- $\mu$ m non-sterile, solvent-resistant polytetrafluoroethylene (PTFE) syringe filter (Fisher Scientific Products, USA). Twenty microliters of the filtrate was injected directly into and analyzed by reverse-phase high-performance liquid chromatography (HPLC) using Waters HPLC e2695 separation module equipped with a photodiode array detector (Waters 2998). A C18 column (Waters symmetry column, 3.5  $\mu$ m, 4.6 $\times$ 75 mm) was used as the stationary phase. The mobile phase composition consisted of pH 7 phosphate buffer and USP/acetonitrile/ethanol (60:20:20 v/v) and had an isocratic flow rate of 0.6 ml/min at 35°C. 5-FU was detected at 264 nm, and Empower 3.0 software was used for data analysis. A calibration curve of pure 5-FU in water was used for quantification. The amount of 5-FU incorporated in SLNs (entrapment efficiency) was calculated using the following formula:

$$\% \text{Entrapment efficiency} = \frac{\text{Calculated 5-FU content} \times 100}{\text{Theoretical 5-FU content}}$$

### Particle Size Determination

Particle size analysis was performed in a dynamic light scattering instrument (DLS) (Nicomp 380 ZLS, Particle Sizing Systems, CA) after suitably diluting with deionized water. The aqueous SLN dispersion before lyophilization and lyophilized SLNs redispersed in deionized water were taken in disposable borosilicate glass culture tubes (VWR Scientific Products). The particle size was determined by placing the sample-filled tubes in the path of a helium neon laser of wavelength 658 nm at 23°C, and data were collected at a scattering angle of 90°. Three measurements of 8 min each were performed, and the

proprietary software available with the instrument was used to calculate the size and expressed as a volume-weighted diameter.

### Zeta Potential Measurements

Zeta potential measurement was performed in the DLS instrument operated in the electrophoretic light scattering mode (ELS) (Nicomp 380 ZLS, Particle Sizing Systems, CA). The SLN dispersion and redispersed lyophilized SLN samples were placed in standard glass cuvettes and the zeta potential measured at 23°C and a scattering angle of  $-14.06^\circ$  using a helium neon laser of wavelength 658 nm. Three measurements of 1 min each were performed to calculate the mean value of zeta potential.

### Differential Scanning Calorimetry (DSC)

Thermal behavior of SLN samples and the physical state of 5-FU in the SLNs were analyzed using a differential scanning calorimeter (PerkinElmer Diamond DSC, CT) equipped with an intercooler 1P. Samples of pure 5-FU, pure GMS, blank lyophilized SLN, and 5-FU-loaded lyophilized SLN were run on DSC. For DSC measurements, 20- $\mu$ l aluminum pans containing 8–10-mg samples were sealed by crimping. The samples were placed in the DSC furnace, and thermograms were recorded by subjecting the samples to a thermal program using a heating rate of 10°C/min in the temperature range from 10 to 350°C under nitrogen purge gas maintained at a flow rate of 20 ml/min. All samples were run in triplicate. The data were analyzed using Pyris Manager (v 1.3) software.

### Fourier Transform Infrared Spectroscopy (FTIR)

The IR spectra were acquired in a Varian Excalibur FTS 4000 FTIR instrument. The samples were spread as a thin layer on a Germanium 45° trough plate and placed in an in-compartment horizontal attenuated total reflectance (HATR) accessory (Pike Technologies, Madison, WI, USA) kept in the sample chamber of the FTIR instrument. The scans were performed over the wavenumber range of 6,000 to 400  $\text{cm}^{-1}$  at a rate of 20 Hz.

### Atomic Force Microscopy (AFM)

AFM studies were done in a Nanosurf easyScan 2 Flex AFM system (Nanosurf AG, Switzerland), and data analyses were performed in the accompanying easyScan 2 software. The instrument was tested for XY calibration using a silicon substrate grid containing an array of silicon oxide squares of height 100 nm separated by 10  $\mu\text{m}$ . An aqueous suspension of a particular sample was placed in circular mica disks (Tedpella Inc., Redding, CA) and equilibrated at room temperature for 24 h. This left a dried sample on the mica disks for analysis. Formulations that were prepared in this manner included aqueous nanosuspension of blank SLNs before lyophilization, aqueous nanosuspension of redispersed lyophilized blank SLNs, aqueous nanosuspension of 5-FU-loaded SLNs before lyophilization, and aqueous nanosuspension of redispersed lyophilized 5-FU-loaded SLNs. The samples were analyzed in the dynamic force tapping mode that enables the

instrument to choose the optimal vibration frequency to be used during measurements. The frequency range that is available for use in this mode is 15 to 500 kHz.

### Transmission Electron Microscopy (TEM)

The shape and internal matrix of individual nanoparticles were visualized using transmission electron microscopy (Hitachi HD-2300 scanning transmission electron microscope, Hitachi High Technologies America, IL). Samples were prepared by placing a drop of the suitably diluted sample onto a Formvar/Carbon 400-mesh copper grid (Ted Pella, CA) and dried at room temperature for 15 min to leave a thin film before removing the excess sample with a lint-free wipe. The prepared grid was equilibrated overnight at room temperature prior to processing *via* TEM. The images were procured in the phase contrast mode.

### *In Vitro* Drug Release Studies from SLNs

*In vitro* drug release studies from lyophilized 5-FU-loaded SLNs were performed in phosphate buffer saline (PBS) of pH 7.4. Four hundred milligrams of lyophilized 5-FU-loaded SLNs was dispersed in 2 ml of PBS (pH 7.4) and placed in a sealed regenerated cellulose membrane bag (dialysis membrane with molecular weight cutoff of 12–14 kDa, Fisherbrand® regenerated cellulose dialysis tubing, 44-mm diameter). The dialysis membrane was then placed in a beaker containing 200 ml of PBS, pH 7.4, and maintained at  $37 \pm 0.5^\circ\text{C}$  in a water bath under magnetic stirring of 100 rpm. At predetermined time intervals, 2-ml samples were withdrawn from the beaker and replaced with fresh PBS. The samples were filtered through a 0.45- $\mu\text{m}$  non-sterile, solvent-resistant PTFE syringe filter (Fisher Scientific Products, USA). Twenty microliters of the filtrate was injected directly into and analyzed by the HPLC method described in the “[Drug Encapsulation Efficiency](#)” section. All experiments were performed in triplicate, and results were reported as mean  $\pm$  standard deviation.

### *In Vitro* Cell Viability Studies in Human Colorectal Adenocarcinoma (Caco-2) Cell Culture

Caco-2 cells (ATCC HTB-37) were grown as a monolayer culture in Eagle’s minimum essential medium (EMEM) (Fisher Scientific, Pittsburg, PA) supplemented with 20% (*v/v*) fetal bovine serum (FBS) containing Earle’s balanced salt solution, non-essential amino acids, 2 mM L-glutamine, 1 mM sodium pyruvate, and 1,500 mg/l sodium bicarbonate. Cells were incubated in 5%  $\text{CO}_2$  atm at 37°C for 96 h. Cells were passaged when 75% confluent by trypsinization (0.05% trypsin-0.02% EDTA solution) and seeded at approximately 50,000 cells per well in sterile, polystyrene 24-well plates (Costar®, USA).

Cells were allowed to adhere for 96 h and media replaced by the appropriate experimental and control formulations for 2 h. Three groups of wells were utilized in this study. One group of wells had cells exposed to nutrient medium, another group of cells was treated to various aliquots of blank SLNs, and the third group of cells was exposed to various aliquots of 5-FU-loaded SLNs. A 1:10 dilution of blank SLN and 5-FU-loaded SLN was prepared separately in DMEM medium.

Five-, ten-, fifteen-, and twenty-microliter aliquots of each were then introduced into wells exposed to a particular treatment. Eight wells received a particular aliquot of the SLN. After 2 h of exposure, each well was washed with 100  $\mu$ l of PBS. The cells were detached by adding 50  $\mu$ l trypsin solution containing 0.05% trypsin and 0.02% EDTA and incubating for 3 min. After 3 min, 200  $\mu$ l EMEM was added, and the contents of each well were transferred to microcentrifuge tubes and centrifuged at 1,000 $\times$ *g* for 5 min. The supernatants were removed and the pellets resuspended in 300  $\mu$ l EMEM. Ten microliters of each dispersion was mixed with 10  $\mu$ l 0.4% trypan blue, and 10  $\mu$ l of this mixture was transferred to a counting slide and observed under Luna automated cell counter (Logos Biosystems, Korea). A one-way ANOVA ( $p < 0.05$ ) was used, and post hoc analysis was performed using Dunnett's *t* test to evaluate the statistical differences between cell viability data between various groups tested.

## RESULTS AND DISCUSSION

### Preparation of SLNs

The aim of this research was to develop SLNs *via* a temperature-modulated solidification process. The particle size of aqueous SLN dispersions was evaluated by DLS to test the influence of various preparation parameters on the particle size. As the amount of lipid in the formulation increased, a concentration-dependent increase in particle size was observed after the lipid concentration exceeded a threshold value. By keeping the surfactant concentration constant and changing the lipid concentration sequentially in trial formulations, it was determined that the minimum quantity of surfactant needed to produce a nanosuspension was twice the parts by weight of the lipid present. A series of lipid/surfactant (*w/w*) mixtures (in the range from 1:2 to 1:5) were prepared and evaluated. The particle size was found to decrease with an increase in surfactant concentration but plateaued off once a critical surfactant concentration was reached. A particle size reduction of up to 20% was observed before leveling off. This is consistent with research reported by other groups and the observation that the presence of surfactant reduces the interfacial tension between the lipid and water and facilitates solid particle formation during the cooling phase of SLN preparation (20). However, the largest particle size observed when the least amount of surfactant was used was 70 $\pm$ 3 nm. This result led to the choice of a composition containing the least amount of surfactant to limit potential surfactant-related toxicities later during cell culture and animal studies. The volume of water used as the dispersion medium did not significantly affect particle size. For a particular lipid/surfactant mixture, the influence of the volume of dispersion medium used was studied by systematically increasing the volume of water in units of 50 ml up to 300 ml. The particle size of the nanosuspension remained at approximately 65 nm through the entire range, demonstrating that the nanosuspension produced from the initial dispersion does not undergo further size change. It was hence noted that the initial lipid/surfactant/water dispersion was possibly a microemulsion and particle size remained unchanged since microemulsions are in principle infinitely dilutable (19). In the optimized formulation, a lipid to surfactant ratio (*w:w*) of 1:2 was used, 150 ml deionized water was used as the dispersion

medium, and the nanosuspension obtained was stirred for 45 min.

Lyophilization is used extensively to recover SLNs from aqueous media by averting possible Ostwald ripening and hydrolysis reaction (4). During lyophilization of aqueous SLN nanosuspensions, cryoprotectants have to be used to preserve the physical integrity of the lipid nanoparticles (21). Cryoprotectants have been shown to reduce aggregation and prevent the SLNs from stress during the freeze-drying process (22). Trehalose was used as the cryoprotectant in the present study since the cryoprotective function of this sugar on SLNs was extensively researched and reported by other researchers (11,23,24). Through trial and error, it was determined that a lipid to trehalose ratio of 1:1 produced solid and free-flowing SLNs following lyophilization of the formulation reported in this work.

### Drug Encapsulation Efficiency

The HPLC method used to quantitate 5-FU was validated according to the ICH guidelines (25). The limit of detection was determined to be 0.22  $\mu$ g and the limit of quantitation was 0.74 microgram. The method was shown to give a linear response over the concentration range of 1.5 to 50  $\mu$ g/ml with a correlation coefficient of 0.9999. The line equation that was developed to calculate the drug in the injected samples was as follows:

$$5\text{-FU in microgram/ml} = (Y + 13,074)/129,136$$

where *Y*=peak area from the chromatogram.

In the present study, the accuracy of the HPLC method was evaluated by a recovery assay through analyses of samples containing known concentration of 5-FU. The mean recovery from the accuracy testing was found to be 100.2% with a relative standard deviation (%RSD) of 0.12. The intraday precision expressed as a mean %RSD was determined to be 0.13 (intraday and interday).

Encapsulation efficiency was observed to be 46% with the three drug amounts (30, 35, and 40 mg 5-FU added per gram GMS) used during SLN preparation. No significant increase in the encapsulation efficiency was observed by increasing the concentration of 5-FU in the lipid, and hence, 30 mg 5-FU was used per gram of GMS in further studies. Such behavior has been reported by other groups when entrapping water-soluble drugs into SLNs (26). 5-FU is hydrophilic and hence may be expected to partition into the aqueous dispersion medium during the preparation of SLNs, producing the observed drug encapsulation efficiency plateau (26). The encapsulation efficiency reported in this work is moderate when compared to other studies, and this may be due to the drug-lipid equilibration process used prior to preparation of SLNs. Hydrophilic molecules in general exhibit low entrapment efficiency in lipid matrices (6,27). Highly water-soluble drugs partition into the aqueous phase during SLN preparation. This aqueous partitioning is primarily responsible for the low entrapment efficiency. Lipid crystallinity also plays an important role in determining the amount of drug ultimately entrapped in the SLNs. When lipids solidify into highly crystalline matrices, the opportunity for drug molecules

to be incorporated within such ordered structures is diminished, leading to low entrapment efficiencies. The encapsulation efficiency of water-soluble drugs in lipid matrices increased when methods such as ionic interaction between counter ions and charged drug molecule (28), conjugation of drug molecule with lipids (29), complexation of drug molecules with ionic polymers (30), and preparation of lipophilic analogs were used (31). The utility of any of these methods in our research remains to be investigated.

### Particle Size

Particle size is a critical parameter for evaluation during and after the formulation of SLNs. The particle size of aqueous blank SLNs before lyophilization was found to be  $65 \pm 23$  nm. The particle size of aqueous 5-FU-loaded SLNs before lyophilization was found to be  $52 \pm 24$  nm. Both particle size distributions contained a second peak at or below approximately 10 nm and are attributed to the presence of Tween 80 micelles. Drug incorporation into the SLNs did not significantly affect the particle size of the resulting formulation. The lyophilization process increased the particle size of both the blank and drug-loaded SLNs, but it remained in the nanometer size range. Figure 1 shows the representative DLS data of the aqueous 5-FU-loaded SLN dispersion before lyophilization. The data shows a bimodal distribution with the peak at  $8 \pm 3$  nm representing Tween 80 micelles, and the peak at  $52 \pm 24$  nm represents the SLNs dispersed in the aqueous medium. The amount of Tween 80 in the formulations is greater than the critical micelle concentration of the surfactant, indicating that the excess surfactant can potentially form micelles in the aqueous medium used in the SLN dispersions. This type of particle size distribution has been reported by Heydenreich *et al.* when preparing and isolating SLNs containing Tween 80 and a cationic lipid (32). The cited work reported Tween 80 micelles at approximately 10 nm, and SLN sizes ranged between 150 and 300 nm depending on the method used for purifying and isolating the SLNs. Figure 2 shows representative DLS data of lyophilized 5-FU-loaded SLNs redispersed in water. The data demonstrates one peak at  $225 \pm 74$  nm representing SLNs. The disappearance of the Tween 80 micelle peak suggests that ultrafiltration that was used to purify SLNs was able to remove excess surfactant from the preparation. The SLNs appear to have undergone an increase in size with the lyophilization process. A moderate increase in particle size of SLNs following lyophilization has been reported by other researchers (33). However, the long-term stability and dispersibility of SLNs have been shown to improve when cryoprotectants such as trehalose are used during lyophilization (34). Similar characteristics were observed in the formulation reported here as well. The lyophilized SLNs possessed particles below the 500-nm size range and dispersed easily when mixed gently with water.

### Zeta Potential

The zeta potential was measured for the blank and drug-loaded aqueous SLN dispersion and lyophilized redispersed SLNs. The zeta potential of the aqueous SLN dispersion prior to lyophilization and lyophilized redispersed blank lipid nanoparticles was approximately  $-15$  mV. GMS is a fatty acid ester

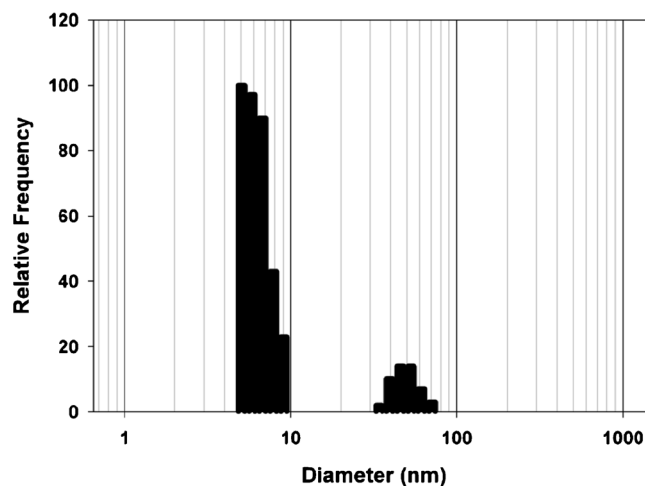


Fig. 1. Representative DLS data of the aqueous 5-FU-loaded SLN dispersion before lyophilization

that may be expected to impart a negative surface charge on the lipid particles, and thus, the blank SLN formulation possesses an overall negative zeta potential. The zeta potential for 5-FU-loaded SLN dispersion was found to be  $-11$  mV, and the zeta potential for redispersed lyophilized SLNs was approximately  $-25$  mV. According to the classical DLVO theory that explains colloidal stability, factors that influence particle aggregation subjecting it to eventually sediment include solvent potential, attractive potential due to van der Waals interactions, and repulsive potential from electrostatic interactions. Of these factors, electrostatic repulsion is the most widely used method to modulate the stability of colloidal particles, including SLNs (35,36). The aqueous stability of SLNs from our work correlated with the zeta potential of a particular formulation. After preparation, the particle size of the nanoparticles in aqueous SLN dispersion was found to remain below 100 nm up to 24 h. This enabled us to decide how soon the formulation should be subjected to lyophilization in order to recover the SLN product. After lyophilization, when the 5-FU-loaded SLN powder was redispersed in water, the particles remained stable for up to 48 h. This observation supports the notion that the redispersed lyophilized 5-FU-loaded SLN preparation should be used within 48 h of reconstitution.

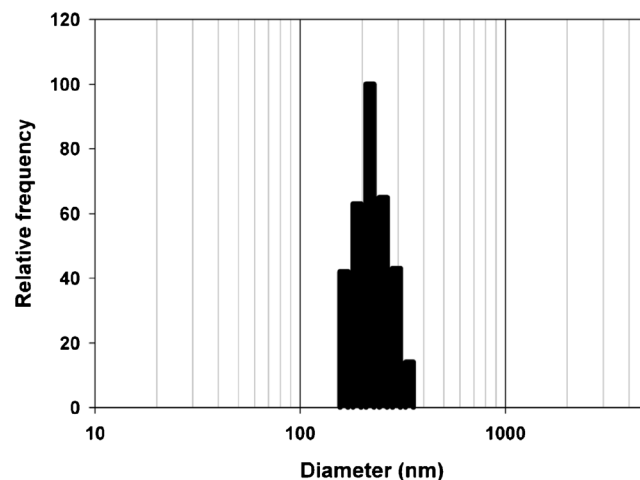


Fig. 2. Representative DLS data of lyophilized 5-FU-loaded SLNs redispersed in water

## DSC

The DSC thermograms of pure GMS (labeled a), pure 5-FU (labeled b), lyophilized blank SLN (labeled c), and lyophilized 5-FU-loaded SLNs (labeled d) are presented in Fig. 3. Pure GMS exhibits an endothermic thermal event attributed to GMS melting with an onset of 65°C and a peak temperature of 71°C (enthalpy of melting=158 J/g). Both the lyophilized blank and 5-FU-loaded SLN samples exhibited a thermal event corresponding to GMS melting at an onset of 51°C and a peak temperature of 61°C. The enthalpy of melting of GMS in lyophilized blank SLNs was 29 J/g, and that of lyophilized 5-FU-loaded SLNs was 27 J/g. The broadening of the GMS melting peak in SLNs suggests a potential decrease in crystallinity of GMS in the nanoparticles. The decrease in the onset and maximum temperatures associated with GMS melting can be attributed to the reduction in particle size and corresponding increase in surface area. This leads to a decrease in melting enthalpy when compared to larger particulates, which require more energy to overcome lattice forces (37). The thermogram of pure 5-FU exhibits its melting as a sharp endothermic peak with an onset temperature of 282°C and a peak maximum at 285°C (38). The thermogram of 5-FU-loaded lyophilized SLN shows 5-FU melting in a small endothermic event with an onset temperature of 288°C and a peak maximum at 289°C (enthalpy of melting=19 J/g). This data provides evidence for the presence of entrapped 5-

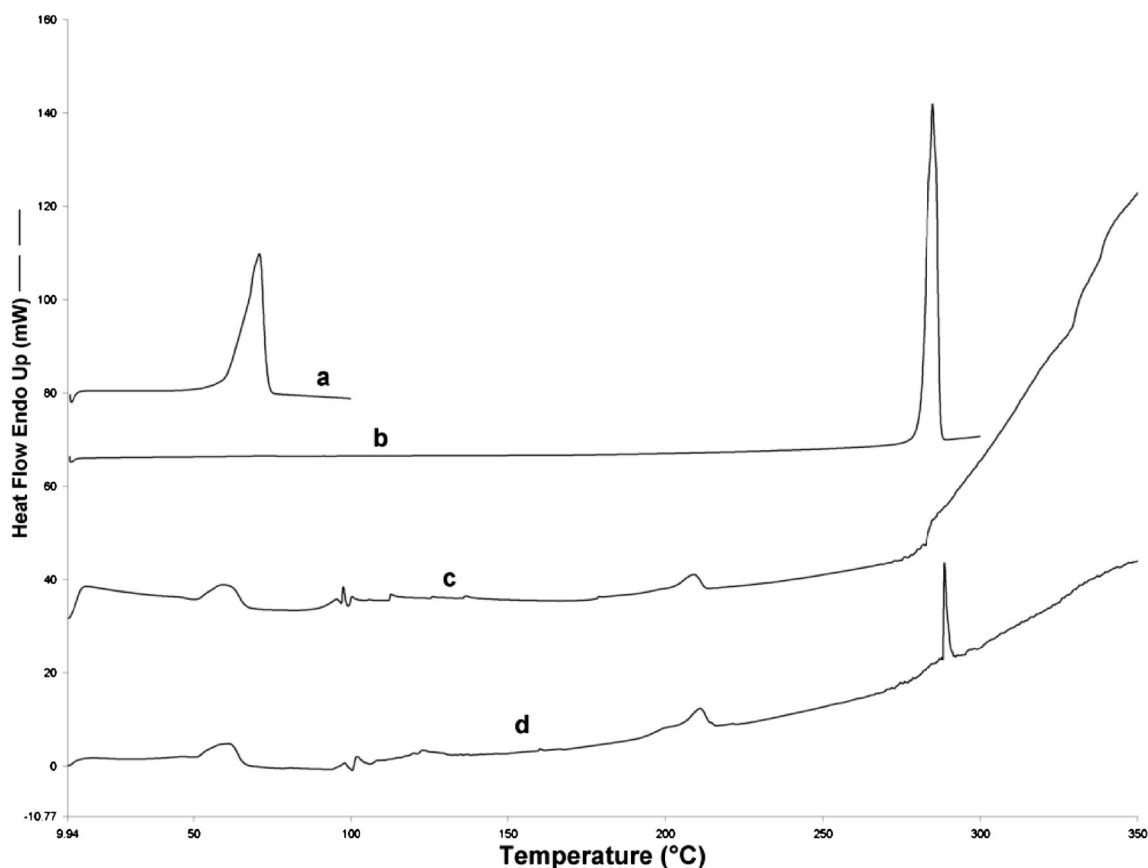


Fig. 3. DSC thermograms of pure GMS (labeled a), pure 5-FU (b), lyophilized blank SLN (c), and lyophilized 5-FU-loaded SLNs (d)

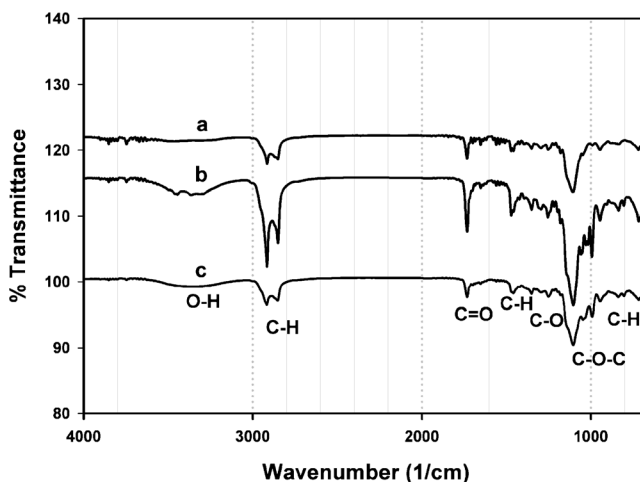
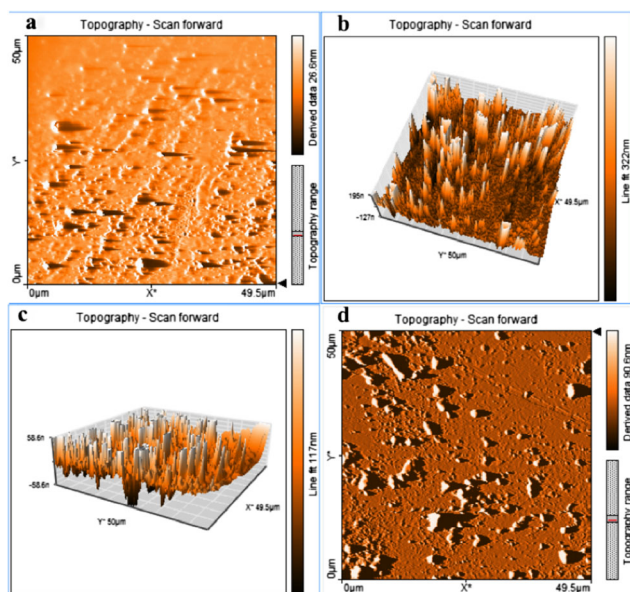


Fig. 4. FTIR spectra of GMS (a), blank SLN (b), and 5-FU SLN (c)

FU in the drug-loaded SLNs and further indicates that a fraction of the drug is present in the crystalline form. Thermal events related to trehalose (cryoprotectant) were found at 100, 111, 121, and 206°C in both the blank and drug-loaded SLNs (39). DSC thermograms for the lyophilized SLN samples show an endothermic peak (endothermic overshoot) at approximately 350°C due to the physical aging phenomena near the glass transition temperature for trehalose (40).



**Fig. 5.** AFM images. **a** Topography scan of the aqueous dispersion of blank SLNs before lyophilization. **b** 3D projection of lyophilized blank SLNs. **c** Line fit AFM image of 5-FU-loaded SLNs before lyophilization. **d** Topography scan image of 5-FU-loaded lyophilized SLNs

## FTIR

Wartewig and Neubert (41) have reviewed the use of FTIR and Raman spectroscopy in pharmaceutical applications. In drug delivery, FTIR-ATR has been used to study drug permeability, drug release, and drug penetration into the stratum corneum. The method was also adapted to obtain information related to

crystallinity of nanostructured lipid carriers (42). Figure 4 shows the FTIR spectra of GMS (a), blank SLN (b), and 5-FU-loaded SLN (c). The peaks at 2,915 and 2,852  $\text{cm}^{-1}$  are attributed to the C–H stretch in the  $-\text{CH}_2$  groups present in the acyl chain of the fatty acid. The absorption band at 1,733  $\text{cm}^{-1}$  is characteristic of C=O stretching that is attributed to the carbonyl group present in the fatty acid ester. The peak at 1,106  $\text{cm}^{-1}$  is due to the C–O–C stretching in the polar head group. Another characteristic band is seen at 3,300  $\text{cm}^{-1}$ , which is due to O–H stretching from the unesterified hydroxyl groups in the polar head group of the glycerol moiety. The band visible at 1,250  $\text{cm}^{-1}$  is due to C–O stretch. The bands at 1,457 and 718  $\text{cm}^{-1}$  are attributed to C–H stretching in the long aliphatic chain of the fatty acid moiety. The position, intensity, and shape of these characteristic IR bands were used by Lin *et al.* to elucidate molecular, conformational, and structural information related to SLNs (8,42). When the IR spectra of GMS are compared to those of blank SLN and 5-FU-loaded SLN, no significant change in position, shape, or intensity of peaks related to GMS is seen. This implies that the lipid is solidifying in the SLNs into a matrix that is similar in structure to that of the original excipient. This finding has implications on the nature and degree of drug release from the 5-FU-loaded SLNs.

## AFM STUDIES

All samples demonstrated the presence of spherical and near-spherical particles. AFM images of the aqueous SLN dispersion containing 5-FU and not containing 5-FU indicated the presence of particles with a mean size below 100 nm. In Fig. 5a, which is the topography scan of the aqueous dispersion of blank SLNs before lyophilization, discrete spherical particles can be seen along with some aggregates. These

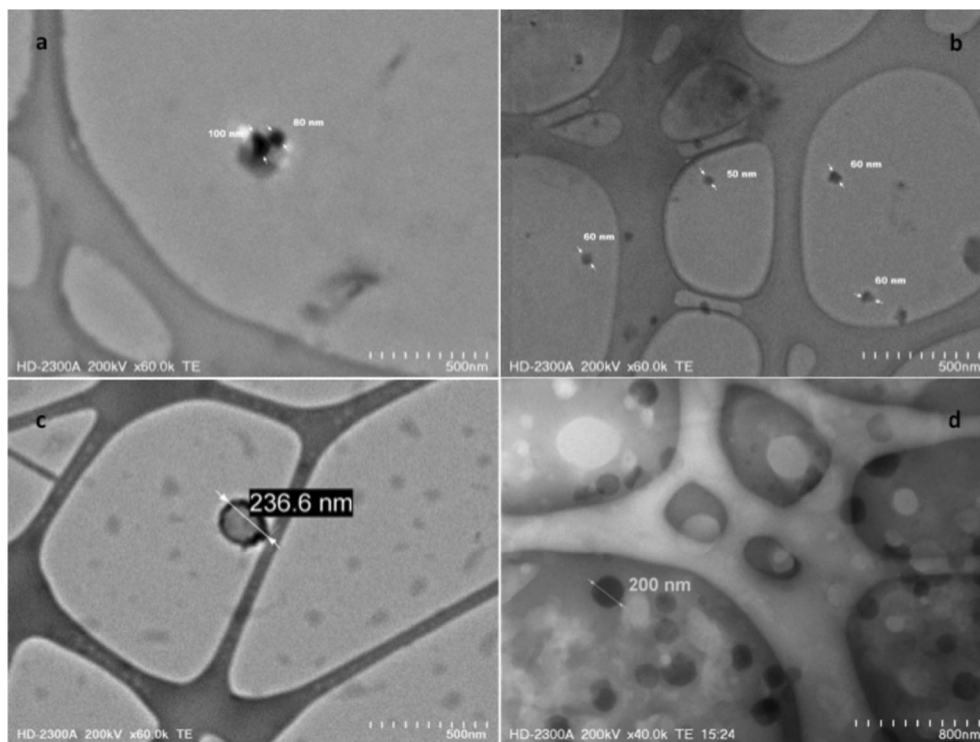


**Fig. 6.** TEM images of SLNs. **a** Blank SLN before lyophilization. **b** 5-FU-loaded SLNs before lyophilization. **c** Blank SLN after lyophilization. **d** 5-FU-loaded SLNs after lyophilization

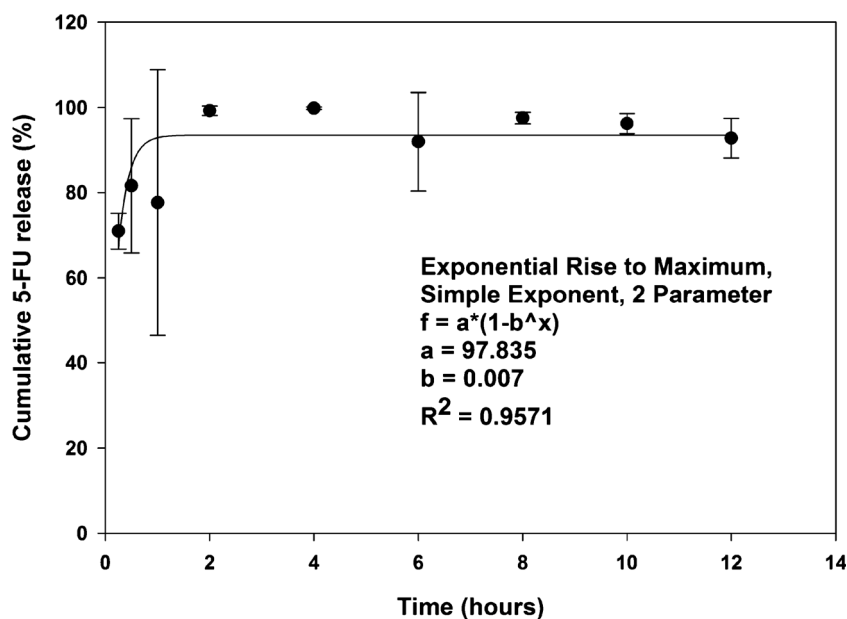


Fig. 7. *In vitro* drug release data from SLNs

aggregates were not recorded in the DLS measurements, indicating that these may have formed during the AFM sample preparation stage. During sample preparation, a drop of a particular nanosuspension was placed in circular mica plates kept in a plastic chamber and allowed to dry at room temperature. Due to the presence of the surfactant and low interfacial tension, it is possible that several particles clustered together when the sample was drying. Figure 5b shows the AFM data obtained from lyophilized blank SLNs. The image is a 3D projection of AFM data that has been processed using the line fit filter available in the analysis software. The results confirm DLS data that showed a moderate increase in particle size observed after lyophilization. Figure 5c shows the line fit AFM image of 5-FU-loaded SLNs before lyophilization. The particles are similar in structure and morphology to blank SLNs before lyophilization. The topography scan image of 5-FU-loaded lyophilized SLNs is represented in Fig. 5d. The increase in size observed following the lyophilization process

is visible in this data. The shape and texture of the particles do not appear to be impacted by the presence of 5-FU.

#### TEM

The shape and surface morphology of blank and 5-FU-loaded SLN dispersion and redispersed lyophilized SLNs were studied using TEM. The TEM images of representative samples are shown in Fig. 6a–d. The size of the SLN samples was found to concur with the particle size distribution data obtained from DLS experiments. All the lipid nanoparticles were found to be more or less spherical in shape with a well-defined periphery. In Fig. 6a, the SLNs visible in the field of view are below 100 nm, as is the case in Fig. 6b. Only dense and solid matrices are seen in TEM images procured in the phase contrast mode, and hence, micelles or any other potential nanostructures formed by the surfactant molecules are not visible. The fibrous material seen in the image is from the ultrathin carbon film on holey carbon support film coating present in the 400-mesh copper TEM grid. The dark spherical structures are the SLNs. TEM images of 5-FU-loaded SLNs have been used by other researchers to analyze the structure of SLNs (43). The lyophilized redispersed blank SLNs appear to be less dense in the core, with a well-defined shell (Fig. 6c). The lyophilized redispersed 5-FU-loaded SLNs demonstrate approximately uniform density throughout the structure, indicating a homogenous lipid matrix (Fig. 6d).

#### *In Vitro* Drug Release Studies

The *in vitro* drug release profile obtained from the dialysis membrane experiment is shown in Fig. 7. The drug release profile was characterized by an initial rapid release of up to 80% within 1 h, followed by continuous release of the drug (44). The initial rapid release may be due to the drug being located on or near the surface of the SLNs and is expected since the SLNs have a large surface to volume ratio because of their small size (44). The drug release beyond 1 h is attributed

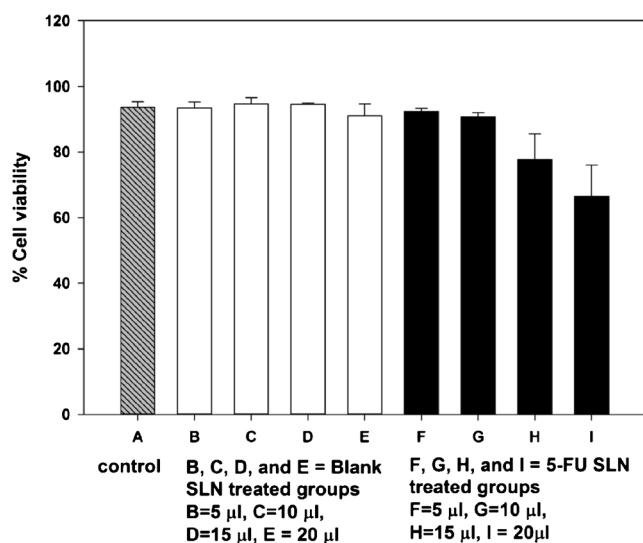


Fig. 8. *In vitro* cell viability data of SLNs in Caco-2 cell culture

to diffusion of the drug dispersed in the lipid matrix (44). Hydrophilic drugs exhibit the tendency to migrate to the aqueous phase during SLN preparation, hence concentrating at or near the surface of the particles exhibiting the initial rapid release. The slower drug release from the SLNs later may be due to the diffusion of the entrapped drug through the lipid matrix (45,46). The initial amount of released 5-FU is desirable to provide a high initial concentration of the drug locally in the cancer cells following administration. The slow and controlled release of the drug subsequently will allow for sustained levels of the chemotherapeutic agent at the cancer site. This may be beneficial therapeutically since SLNs and other small particulates are capable of preferentially accumulating within tumors *via* the enhanced permeability and retention effect (10,47). SLNs undergo degradation in the presence of lipase enzyme, and hence, the 5-FU-loaded SLNs reported here may be acted upon by lipases when administered orally. When cyclosporine-containing SLNs were investigated for potential use in ophthalmic delivery, no drug release was observed *in vitro* in the absence of lipase/colipase complex (48). The formulation demonstrated up to 28% drug release in 90 min when the *in vitro* release study was performed in a pH 7.4 buffer containing lipase/colipase complex. Studies done by Olbrich *et al.* have also established that drug release from SLNs can occur through diffusion and enzymatic degradation of the lipid matrix by lipases (49,50). These studies indicated that the nature of the lipid and surfactants affected the degradation process. An interesting finding in cancer research in recent years has been the identification of lipases such as monoacyl glycerol lipase (MAGL) and their involvement in altered metabolism in cancer cells (51,52). Given the relevance of lipase-mediated biodegradation of SLNs, this new insight into the pathogenesis and proliferation of cancers offers new opportunities for the targeted delivery of therapeutic material *via* SLNs to treat various cancers.

### ***In Vitro* Cell Viability Studies in Caco-2 Cell Culture**

Results from the *in vitro* cell exposure studies performed in Caco-2 cells are shown in Fig. 8. The automated cell counter used in this study is equipped with a 5-MP digital camera that captured the images shown in the figures. The technique utilizes a dye exclusion method to analyze cell viability (53). When cell suspensions are treated with trypan blue stain, viable and living cells do not absorb the dye whereas dead cells are stained blue. This difference in staining is attributed to changes in cell permeability between live and dead cells (54). Cell viability of nutrient medium-treated cells and blank SLN-treated cells was approximately 94% with no statistical differences observed between the groups. This data demonstrates that the blank SLNs was tolerated by the cells and hence may be deemed as biocompatible in Caco-2 cells in the concentration range tested. Other researchers observed similar results when testing SLNs on vaginal epithelial cell lines (6). However, the cells treated with 5-FU-loaded SLN suspensions showed a concentration-dependent decrease in viability. The cells exposed to 5  $\mu$ l drug-loaded SLN dispersion showed 92.4 $\pm$ 0.9% viability. The cell viability of the groups exposed to 10 and 15  $\mu$ l decreased to 90.7 $\pm$ 1.3 and 77.7 $\pm$ 7.8%, respectively. The cell viability of the cells exposed to 20  $\mu$ l further decreased to 66.5 $\pm$ 9.5%. The viability data of 5-FU-loaded SLN-treated cells (15 and 20  $\mu$ l) were statistically

significant ( $p < 0.05$ ) when compared to cells exposed to nutrient medium and blank SLNs. This result indicates that the 5-FU entrapped within the SLN was released and hence produced the observed cell death. Similar concentration-dependent biological effects were observed by other researchers investigating SLNs prepared using stearic acid and cetyl palmitate (35,55). Similarly, paclitaxel- and doxorubicin-loaded SLNs were found to possess significant and potent anticancer effects when tested in *in vitro* cell cultures (12).

### **CONCLUSION**

In this study, SLNs were successfully prepared *via* a temperature-modulated solidification technique. An anticancer drug, 5-FU, was incorporated in the SLNs. The developed technique is simple and reproducible, prepares nanoparticles without the need of high energy and organic solvents, and has the potential to easily scale up for large-scale SLN production. The particle size of SLN dispersion was approximately 66 nm, and that of redispersed lyophilized SLNs was below 500 nm. The SLN dispersions were lyophilized to stabilize the SLNs, and the lyophilizates exhibited good redispersibility when gently mixed with water. Morphological studies using TEM images showed spherical to oval particles with well-defined periphery. A decrease in the enthalpy and onset temperature for the melting point of GMS in the DSC thermograms is consistent with the nanostructure of the SLNs. The drug encapsulation efficiency was found to be approximately 46% and is attributed to the water-soluble nature of 5-FU, leading to rapid partitioning into the aqueous phase and hence decreased encapsulation into the SLNs. *In vitro* drug release studies from redispersed lyophilized SLNs showed that 80% of the encapsulated drug was released within 1 h. *In vitro* cell culture studies demonstrated that the blank SLNs were biocompatible in the concentration ranges tested. 5-FU-loaded SLNs produced a concentration-dependent decrease in cell viability in Caco-2 cell cultures. Future studies in animal models will delineate compatibility and utility of these formulations in biological systems.

### **ACKNOWLEDGMENTS**

This research was performed with support from start-up funds made available by the Department of Pharmacy Practice at the University of Toledo College of Pharmacy and Pharmaceutical Sciences. We are grateful to Dr. Joseph Lawrence, Center for Sensor and Materials Characterization, University of Toledo College of Engineering, for his assistance during the TEM work. We thank Ms. Charisse Montgomery, Scientific Editor and College Communicator, College of Pharmacy and Pharmaceutical Sciences, University of Toledo, for her review and comments.

**Conflict of Interest** The authors report no conflict of interest.

### **REFERENCES**

1. del Pozo-Rodriguez A, Delgado D, Gascon A, Solinis M. Lipid nanoparticles as drug/gene delivery systems to the retina. *J Ocul Pharmacol Ther.* 2013;29(2):173–88.

2. Genç L, Dikmen G, Güneş G. Formulation of nano drug delivery systems. *J Mater Sci Eng A*. 2011;1(1):132–7.
3. Pradhan M, Singh D, Singh M. Novel colloidal carriers for psoriasis: current issues, mechanistic insight and novel delivery approaches. *J Control Release*. 2013;170(3):380–95.
4. Mehnert W, Mäder K. Solid lipid nanoparticles: production, characterization and applications. *Adv Drug Deliv Rev*. 2001;47(2–3):165–96.
5. Basu B, Garala K, Bhalodia R, Joshi B, Mehta K. Solid lipid nanoparticles: a promising tool for drug delivery system. *J Pharm Res*. 2010;3(1):84–92.
6. Alukda D, Sturgis T, Youan B-BC. Formulation of tenofovir-loaded functionalized solid lipid nanoparticles intended for HIV prevention. *J Pharm Sci*. 2011;100(8):3345–56.
7. Qi J, Lu Y, Wu W. Absorption, disposition and pharmacokinetics of solid lipid nanoparticles. *Curr Drug Metab*. 2012;13(4):418–28.
8. Li XW, Lin XH, Zheng LQ, Yu L, Lv FF, Zhang QQ, *et al*. Effect of poly(ethylene glycol) stearate on the phase behavior of monopalmitate/Tween80/water system and characterization of poly(ethylene glycol) stearate-modified solid lipid nanoparticles. *Colloids Surf A Physicochem Eng Asp*. 2008;317(1–3):352–9.
9. Siekmann B, Westesen K. Investigations on solid lipid nanoparticles prepared by precipitation in o/w emulsions. *Eur J Pharm Biopharm*. 1996;42(2):104–9.
10. Reddy LH, Sharma RK, Chuttani K, Mishra AK, Murthy RSR. Influence of administration route on tumor uptake and biodistribution of etoposide loaded solid lipid nanoparticles in Dalton's lymphoma tumor bearing mice. *J Control Release*. 2005;105(3):185–98.
11. Cavalli R, Caputo O, Gasco MR. Preparation and characterization of solid lipid nanospheres containing paclitaxel. *Eur J Pharm Sci*. 2000;10(4):305–9.
12. Serpe L, Catalano MG, Cavalli R, Ugazio E, Bosco O, Canaparo R, *et al*. Cytotoxicity of anticancer drugs incorporated in solid lipid nanoparticles on HT-29 colorectal cancer cell line. *Eur J Pharm Biopharm*. 2004;58(3):673–80.
13. Howlader N NA, Krapcho M, Neyman N, Aminou R, Waldron W, Altekruse SF, Kosary CL, Ruhl J, Tatalovich Z, Cho H, Mariotto A, Eisner MP, Lewis DR, Chen HS, Feuer EJ, Cronin KA, Edwards BK (Eds). SEER cancer statistics review 1975–2008. Bethesda, MD: National Cancer Institute, NIH, DHHS.
14. Cancer Trends Progress Report—2009/2010 update. Bethesda, MD: National Cancer Institute, NIH, DHHS, April 2010.
15. Carethers JM, Smith EJ, Behling CA, Nguyen L, Tajima A, Doctolero RT, *et al*. Use of 5-fluorouracil and survival in patients with microsatellite-unstable colorectal cancer. *Gastroenterology*. 2004;126(2):394–401.
16. Sander CA, Pfeiffer C, Kligman AM, Plewig G. Chemotherapy for disseminated actinic keratoses with 5-fluorouracil and isotretinoin. *J Am Acad Dermatol*. 1997;36(2):236–8.
17. Longley DB, Johnston PG. 5-Fluorouracil. Apoptosis, cell signaling, and human diseases. 2007:263–78.
18. Diasio RB, Harris BE. Clinical pharmacology of 5-fluorouracil. *Clin Pharmacokinet*. 1989;16(4):215–37.
19. Prince LM. Microemulsions versus micelles. *J Colloid Interface Sci*. 1975;52(1):182–8.
20. Zhang J, Fan Y, Smith E. Experimental design for the optimization of lipid nanoparticles. *J Pharm Sci*. 2009;98(5):1813–9.
21. Izutsu K, Kojima S. Excipient crystallinity and its protein-structure-stabilizing effect during freeze-drying. *J Pharm Pharmacol*. 2002;54(8):1033–9. Epub 2002/08/28.
22. Shahgaldian P, Gualbert J, Aissa K, Coleman AW. A study of the freeze-drying conditions of calixarene based solid lipid nanoparticles. *Eur J Pharm Biopharm*. 2003;55(2):181–4. Epub 2003/03/15.
23. Schwarz C, Mehnert W. Freeze-drying of drug-free and drug-loaded solid lipid nanoparticles (SLN). *Int J Pharm*. 1997;157(2):171–9. Epub 1999/09/09.
24. Heiati H, Tawashi R, Phillips NC. Drug retention and stability of solid lipid nanoparticles containing azidothymidine palmitate after autoclaving, storage and lyophilization. *J Microencapsul*. 1998;15(2):173–84.
25. Validation of analytical procedures: text and methodology Q2(R1). ICH Harmonised Tripartite Guideline: International Conference on Harmonisation of Technical Requirements for Registration of Pharmaceuticals for Human Use; 1994.
26. Singh S, Dobhal AK, Jain A, Pandit JK, Chakraborty S. Formulation and evaluation of solid lipid nanoparticles of a water soluble drug: zidovudine. *Chem Pharm Bull*. 2010;58(5):650–5.
27. Schubert MA, Mueller-Goymann CC. Characterisation of surface-modified solid lipid nanoparticles (SLN): influence of lecithin and nonionic emulsifier. *Eur J Pharm Biopharm*. 2005;61(1–2):77–86.
28. Cavalli R, Caputo O, Gasco MR. Solid lipospheres of doxorubicin and idarubicin. *Int J Pharm*. 1993;89(1):R9–R12.
29. Olbrich C, Gessner A, Kayser O, Müller RH. Lipid-drug-conjugate (LDC) nanoparticles as novel carrier system for the hydrophilic antitrypanosomal drug diminazenediacetate. *J Drug Target*. 2002;10(5):387–96.
30. Wong HL, Bendayan R, Rauth AM, Wu XY. Development of solid lipid nanoparticles containing ionically complexed chemotherapeutic drugs and chemosensitizers. *J Pharm Sci*. 2004;93(8):1993–2008.
31. Wang J-X, Sun X, Zhang Z-R. Enhanced brain targeting by synthesis of 3',5'-diocanoyl-5-fluoro-2'-deoxyuridine and incorporation into solid lipid nanoparticles. *Eur J Pharm Biopharm*. 2002;54(3):285–90.
32. Heydenreich A, Westmeier R, Pedersen N, Poulsen H, Kristensen H. Preparation and purification of cationic solid lipid nanospheres—effects on particle size, physical stability and cell toxicity. *Int J Pharm*. 2003;254(1):83–7.
33. Yang SC, Zhu JB. Preparation and characterization of camptothecin solid lipid nanoparticles. *Drug Dev Ind Pharm*. 2002;28(3):265–74.
34. del Pozo-Rodriguez A, Solinis MA, Gascon AR, Pedraz JL. Short- and long-term stability study of lyophilized solid lipid nanoparticles for gene therapy. *Eur J Pharm Biopharm*. 2009;71(2):181–9.
35. Asasutjarit R, Lorenzen S-I, Sirivichayakul S, Ruxrungtham K, Ruktanonchai U, Ritthidej GC. Effect of solid lipid nanoparticles formulation compositions on their size, zeta potential and potential for in vitro pHIS-HIV-hugag transfection. *Pharm Res*. 2007;24(6):1098–107.
36. de Faria TJ, Souza-Silva E, de Oliveira DT, Senna Elenara L, Tonussi CR. Evaluation of the pro-inflammatory potential of nanostructured drug carriers in knee-joints of rats: effect on nociception, edema, and cell migration. *J Pharm Sci*. 2009;98(12):4844–51.
37. Li Z, Yu L, Zheng L, Geng F. Studies on crystallinity state of puerarin loaded solid lipid nanoparticles prepared by double emulsion method. *J Therm Anal Calorim*. 2010;99(2):689–93.
38. Yassin Alaa Eldeen B, Anwer MD K, Mowafy Hammam A, El-Bagory Ibrahim M, Bayomi Mohsen A, Alsarra Ibrahim A. Optimization of 5-fluorouracil solid-lipid nanoparticles: a preliminary study to treat colon cancer. *Int J Med Sci*. 2010;7(6):398–408.
39. Sussich F, Bortoluzzi S, Cesàro A. Trehalose dehydration under confined conditions. *Thermochim Acta*. 2002;391(1):137–50.
40. Simperler A, Kornherr A, Chopra R, Bonnet PA, Jones W, Motherwell WDS, *et al*. Glass transition temperature of glucose, sucrose, and trehalose: an experimental and in silico study. *J Phys Chem B*. 2006;110(39):19678–84.
41. Wartewig S, Neubert RHH. Pharmaceutical applications of Mid-IR and Raman spectroscopy. *Adv Drug Deliv Rev*. 2005;57(8):1144–70.
42. Lin X, Li X, Zheng L, Yu L, Zhang Q, Liu W. Preparation and characterization of monopalmitate nanostructured lipid carriers. *Colloids Surf A Physicochem Eng Asp*. 2007;311(1–3):106–11.
43. Liu D, Ge Y, Tang Y, Yuan Y, Zhang Q, Li R, *et al*. Solid lipid nanoparticles for transdermal delivery of diclofenac sodium: preparation, characterization and in vitro studies. *J Microencapsul*. 2010;27(8):726–34.
44. Li XM, Xu YL, Chen GG, Wei P, Ping QN. PLGA nanoparticles for the oral delivery of 5-fluorouracil using high pressure homogenization-emulsification as the preparation method and in vitro/in vivo studies. *Drug Dev Ind Pharm*. 2008;34(1):107–15.
45. Jain SK, Chaurasiya A, Gupta Y, Jain A, Dagur P, Joshi B, *et al*. Development and characterization of 5-FU bearing ferritin appended solid lipid nanoparticles for tumour targeting. *J Microencapsul*. 2008;25(5):289–97.
46. Glavas-Dodov M, Fredro-Kumbaradzi E, Goracinova K, Simonoska M, Calis S, Trajkovic-Jolevska S, *et al*. The effects of

- lyophilization on the stability of liposomes containing 5-FU. *Int J Pharm.* 2005;291(1):79–86.
47. Matsumura Y, Maeda H. A new concept for macromolecular therapeutics in cancer chemotherapy: mechanism of tumorotropic accumulation of proteins and the antitumor agent smancs. *Cancer Res.* 1986;46(12, Pt. 1):6387–92.
  48. Gokce EH, Sandri G, Bonferoni MC, Rossi S, Ferrari F, Gueneri T, *et al.* Cyclosporine A loaded SLNs: evaluation of cellular uptake and corneal cytotoxicity. *Int J Pharm.* 2008;364(1):76–86.
  49. Olbrich C, Kayser O, Mueller RH. Enzymatic degradation of Dynasan 114 SLN—effect of surfactants and particle size. *J Nanoparticle Res.* 2002;4(1/2):121–9.
  50. Olbrich C, Kayser O, Muller RH. Lipase degradation of Dynasan 114 and 116 solid lipid nanoparticles (SLN)—effect of surfactants, storage time and crystallinity. *Int J Pharm.* 2002;237(1–2):119–28.
  51. Nomura DK, Lombardi DP, Chang JW, Niessen S, Ward AM, Long JZ, *et al.* Monoacylglycerol lipase exerts dual control over endocannabinoid and fatty acid pathways to support prostate cancer. *Chem Biol.* 2011;18(7):846–56. Cambridge, MA, United States.
  52. Nomura DK, Long JZ, Niessen S, Hoover HS, Ng S-W, Cravatt BF. Monoacylglycerol lipase regulates a fatty acid network that promotes cancer pathogenesis. *Cell.* 2010;140(1):49–61. Cambridge, MA, United States.
  53. Eytan GD, Regev R, Oren G, Hurwitz CD, Assaraf YG. Efficiency of P-glycoprotein-mediated exclusion of rhodamine dyes from multidrug-resistant cells is determined by their passive transmembrane movement rate. *Eur J Biochem.* 1997;248(1):104–12.
  54. Guo H, Hao R, Wei Y, Sun D, Sun S, Zhang Z. Optimization of electrotransfection conditions of mammalian cells with different biological features. *J Membr Biol.* 2012;245(12):789–95.
  55. Olbrich C, Gessner A, Schroder W, Kayser O, Muller RH. Lipid-drug conjugate nanoparticles of the hydrophilic drug diminazene-cytotoxicity testing and mouse serum adsorption. *J Control Release Off J Control Release Soc.* 2004;96(3):425–35.